Nuclear Instruments and Methods in Physics Research B 317 (2013) 492–500

Contents lists available at ScienceDirect

Nuclear Instruments and Methods in Physics Research B

journal homepage: www.elsevier.com/locate/nimb

Recent exploits of the ISOLTRAP mass spectrometer

S. Kreim [a,b,*], D. Atanasov [b], D. Beck [c], K. Blaum [b], Ch. Böhm [b], Ch. Borgmann [b], M. Breitenfeldt [d], T.E. Cocolios [a,e], D. Fink [b,f], S. George [b], A. Herlert [g], A. Kellerbauer [b], U. Köster [h], M. Kowalska [a], D. Lunney [i], V. Manea [i], E. Minaya Ramirez [c,j], S. Naimi [b], D. Neidherr [c], T. Nicol [k], R.E. Rossel [l,m], M. Rosenbusch [n], L. Schweikhard [n], J. Stanja [o], F. Wienholtz [n], R.N. Wolf [n], K. Zuber [o]

[a] CERN, CH-1211 Geneva, Switzerland
[b] Max-Planck-Institut für Kernphysik, Saupfercheckweg 1, 69117 Heidelberg, Germany
[c] GSI Helmholtzzentrum für Schwerionenforschung GmbH, 64291 Darmstadt, Germany
[d] KU Leuven, 3001 Leuven, Belgium
[e] University of Manchester, Manchester M13 9PL, United Kingdom
[f] Fakult ät f"ur Physik und Astronomie, Ruprecht-Karls-Universität, 69120 Heidelberg, Germany
[g] FAIR GmbH, 64291 Darmstadt, Germany
[h] Institut Laue Langevin, 38042 Grenoble, France
[i] CSNSM-IN2P3-CNRS, Université Paris-Sud, 91406 Orsay, France
[j] Helmholtz-Institut Mainz, 55099 Mainz, Germany
[k] ENSICAEN, 14000 Caen, France
[l] Institut für Physik, Johannes Gutenberg-Universität, Mainz, Germany
[m] Hochschule RheinMain, Fachbereich Design Informatik Medien, D-65197 Wiesbaden, Germany
[n] Institut für Physik, Ernst-Moritz-Arndt-Universität, 17487 Greifswald, Germany
[o] Technische Universität Dresden, 01069 Dresden, Germany

ARTICLE INFO

Article history:
Received 21 March 2013
Received in revised form 2 July 2013
Accepted 3 July 2013
Available online 28 August 2013

Keywords:
Penning-trap mass spectrometry
Beam purification
Measurement of pure ion ensembles
Multi-reflection time-of-flight mass separator
Ion-beam analysis

ABSTRACT

The Penning-trap mass spectrometer ISOLTRAP, located at the isotope-separator facility ISOLDE (CERN), is presented in its current form taking into account technical developments since 2007. Three areas of developments are presented. The reference ion sources have been modified to guarantee a sufficient supply of reference ions for mass measurements and systematic studies. Different excitation schemes have been investigated for manipulation of the ion motion in the Penning trap, to enhance either the purification or measurement process. A multi-reflection time-of-flight mass separator has been implemented and can now be routinely used for purification and as a versatile tool for beam analysis.

1. Introduction

The ISOLTRAP setup has been used to perform Penning-trap mass spectrometry on pure samples of exotic nuclides for over two decades and has determined the mass of close to 600 short-lived nuclides [1]. Mass measurements allow probing nuclear structure, answering questions of astrophysical relevance, and are needed for tests of fundamental symmetries or theories. A recent example is the mass measurement of ^{82}Zn which is important for modelling the crustal composition of neutron stars. Through the precise mass value from a Penning-trap measurement it was possible to clarify that ^{82}Zn is not present in the outer crust of a neutron star according to [2,3]. A general overview of Penning-trap mass spectrometry can be found for example in [4,5]. A compilation of recent results of the ISOLTRAP experiment is published in [6].

The ISOLTRAP experiment is located at the isotope-separator facility ISOLDE at CERN, where thick, heated targets are bombarded with a 1.4–GeV proton pulse [7]. The ISOL technique provides a low-energy, radioactive beam. After diffusion from the target, the beam passes the transfer line (i. e. ion source), which typically delivers singly-charged ions. In most cases, the beam is purified by a separator magnet with a resolving power on the order of $R = m/\Delta m \approx 10^3$ suppressing neighboring isotopes. Challenging experimental conditions for weakly produced exotic isotopes

* Corresponding author at: CERN, CH-1211 Geneva, Switzerland. Tel.: +41 0227672646.
E-mail address: skreim@cern.ch (S. Kreim).

0168-583X/$ - see front matter © 2013 Elsevier B.V. All rights reserved.
http://dx.doi.org/10.1016/j.nimb.2013.07.072

require the continuous development of new experimental techniques. Previously, the Penning-trap mass spectrometer ISOLTRAP consisted of three ion traps, two for preparation and purification of the delivered nuclides and a precision Penning trap for the actual mass measurement using the time-of-flight ion-cyclotron-resonance (TOF-ICR) technique [8]. The multi-reflection time-of-flight mass separator (MR-TOF MS) was installed in 2010 as an auxiliary purification device [9].

Many exotic isotopes of interest have half-lives as low as some tens of milliseconds and a minute production rate, but are often contaminated by (orders of magnitude) higher-yield isobaric masses. Focus has thus been laid on three aspects: gain in precision, reduction of overall measurement time, and efficient preparation of pure radioactive samples for state-of-the-art mass measurements or spectroscopic experiments. The current ISOLTRAP setup will be presented in Section 2 including the technical developments on the reference ion sources. Section 3 will cover new excitation schemes for the manipulation of the ion motion within the Penning trap with the goal of higher precision or purification of the ion ensemble at higher resolving power. In addition, Section 4 focuses on the use of the MR-TOF MS as a diagnostic tool for ion-beam analysis. A tape-station setup has also been implemented to perform decay-assisted mass measurements and trap-assisted decay spectroscopy [10]. Where applicable, the ISOLTRAP results discussed here will be put in context with similar developments of other experiments or facilities.

2. The current ISOLTRAP setup

Fig. 1 shows the current setup, where the grey-shaded parts have been enhanced or implemented within the scope of this work. The ISOLTRAP setup consists of four traps, see Fig. 1: a linear segmented radio-frequency quadrupole ion beam cooler and buncher (RFQ) for beam preparation (RFQ cooler and buncher), the multi-reflection time-of-flight mass separator (MR-TOF MS) recently commissioned on-line, and two Penning traps (preparation and precision Penning trap) [8,9]. The RFQ is located on a floatable high-voltage platform to match the energy of the incoming 30–60 keV ISOLDE ion beam. The remaining few electronvolts kinetic energy are cooled via collisions with helium buffer gas in a few milliseconds [11]. After a sufficient number of ions are accumulated, they are ejected towards a pulsed drift tube (1st deceleration cavity) which accelerates and transfers them to their nominal kinetic energy of E_{ini} = 3.1 keV with respect to ground. The resulting ion bunch exhibits a peak width of about $\Delta t_{FHWM} \approx 60$ ns and a kinetic-energy spread of about $\Delta E_{kin}^{90\%} \approx 60$ eV [12]. Upon injection into the MR-TOF MS, the so-called in-trap lift (trapping cavity) reduces the kinetic energy of the ion ensemble for trapping to $E_{kin}^{MR-TOFMS} = 2.1$ keV [13]. Isobaric contaminants are then separated due to mass-over-charge dependent flight times after repeated oscillations between electrostatic mirrors, reaching comparable resolving powers as purification in Penning traps but within an order of magnitude less time. The MR-TOF mass separator can thus act as an auxiliary device for isobaric purification reaching resolving powers on the order of $R = m/\Delta m \approx 10^5$ within a few ten milliseconds. For a detailed discussion on the technical characterization, see [12]. Subsequent to the time-of-flight separation, the ion ensemble is re-accelerated to the initial energy of $E_{ini} = 3.1$ keV and passes the Bradbury-Nielsen gate (BN gate) [14]. The gate has been installed directly behind the MR-TOF mass separator and reaches a suppression factor for contaminating ions of four orders of magnitude, thus considerably enhancing the performance of ISOLTRAP when dealing with large contamination ratios [9]. The ions of interest are transferred to the preparation Penning trap, in front of which a final pulsed drift tube (2nd deceleration cavity) reduces the kinetic energy of the ion ensemble to a value which allows capture in the preparation Penning trap. A

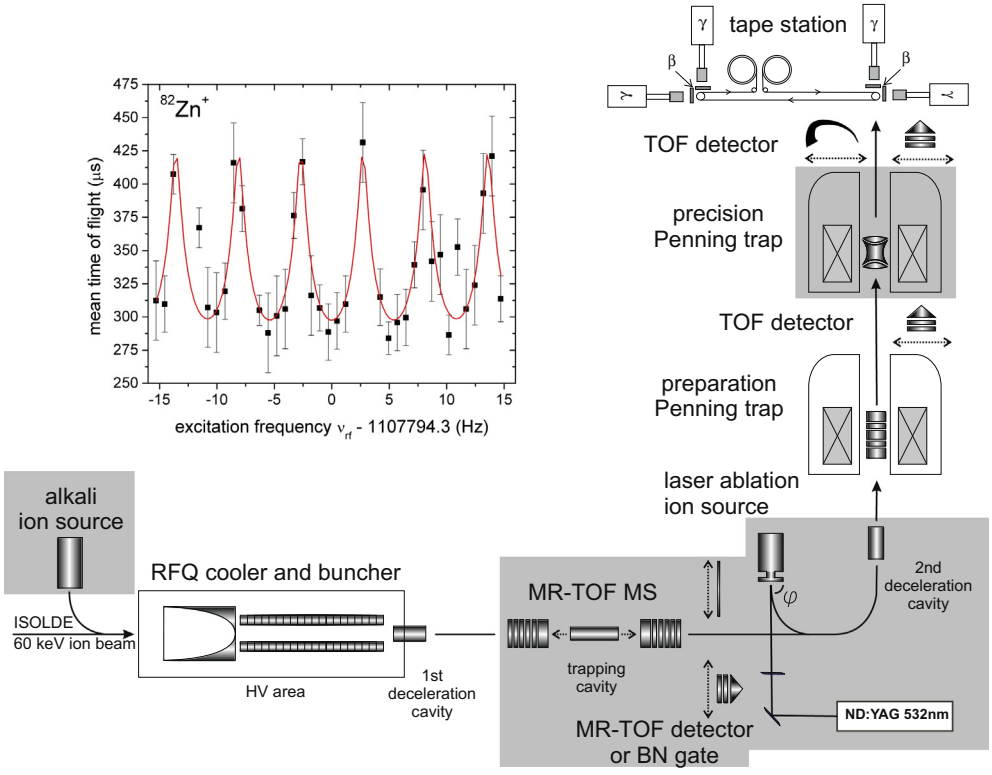

Fig. 1. Schematic view of the ISOLTRAP setup. Parts marked in grey have been enhanced or implemented within the scope of this work. The inset shows a Ramsey time-of-flight resonance of $^{82}Zn^{+}$. For details, see text.

typical value of $E_{kin}^{trap} \approx 80$ eV could be determined by analyzing the energy distribution. In the preparation Penning trap, the ions are cooled by mass-selective resonant buffer-gas centering and contaminants can be further removed [15]. This technique typically reaches resolving powers between $R = 10,000$ and $R = 100,000$ on a time scale ranging from one to a few hundred ms. A purified sample is then sent to the precision Penning trap for the actual measurement.

In the precision Penning trap, the TOF-ICR technique is employed to determine the cyclotron frequency ν_c of a stored ion by measuring its flight time to a TOF detector above the trap, (see Fig. 1).

$$\nu_c = \frac{1}{2\pi}\frac{q}{m}\cdot B, \tag{1}$$

where m (q) denotes the mass (charge) of the ion and B the magnetic field. This technique exploits the fact that the cyclotron frequency ν_c is the sum of the frequencies of the two radial eigenmotions of the stored ion, the modified cyclotron frequency ν_+ and the magnetron frequency ν_-, and the two motions can be converted into each other by applying a quadrupolar radio-frequency (RF) field at the sum frequency $\nu_c = \nu_+ + \nu_-$ [16]. From Eq. (1) the atomic mass can be extracted from the measurement on ions and in conjunction with a reference frequency measurement of a well known reference species with mass m_{ref} [17–19]:

$$m = \frac{\nu_c^{ref}}{\nu_c}(m_{ref} - m_e) + m_e. \tag{2}$$

Here, m_e denotes the electron mass.

Reference Ion Sources The reference ions are usually supplied by an alkali ion source, which is installed in front of the entrance to the ISOLTRAP buncher and is shown on the left of Fig. 2. This ion source provides the alkali isotopes $^{39,41}K^+$, $^{85,87}Rb^+$, and $^{133}Cs^+$ and is implemented at the ISOLTRAP experiment on the same reference potential as the buncher. It contains a commercial pellet which is heated to a temperature of about 1000°C and provides a continuous ion beam with a surplus of roughly 30 eV energy to the reference potential. As an alternative, a laser-ablation ion source can be used for provision of reference ions. Since its first use in 2002 [20], the laser-ablation ion source has been modified several times. A recent series of changes has been applied to allow for high-precision Q-value measurements of the possible neutrinoless double β-decay from ^{110}Pd to ^{110}Cd [21], the most important being the change of the angle between the pellet and the laser beam, which is now $\varphi = 90°$, see Fig. 1. In the current design (as seen in Fig. 2 on the right) the extraction geometry is manufactured in such a way as to resemble a Pierce geometry [22]. The potential of the pellet (usually pellets of glassy carbon, in the case of the measurements mentioned above a threefold pellet of carbon, palladium, and cadmium) is matched to the reference potential of the RFQ ion trap, ensuring the possibility of fast switching between an on-line and reference mass measurement without having to change transport voltages. The frequency-doubled Nd:YAG laser beam (wavelength of 532 nm, pulse length of roughly 3 ns and pulse energy of up to 72 mJ) is shot on the pellet. Focused to a radius at the pellet of only 1.4 mm (pulse-power density of 5×10^7 mm) a plasma environment is generated, from which the carbon ions are extracted. After such a laser-ablation pulse, an ion cloud of various cluster sizes $^{12}C_n$ is transported at an energy of 3.1 keV towards the preparation Penning trap. The temporal spread of the different clusters is so small that clusters of more than one mass value are decelerated by the second deceleration cavity and subsequently captured in the preparation Penning trap. This circumstance has made the application of the mass-selective resonant buffer-gas centering technique cumbersome due to the Coulomb interaction of the different species in the trap. The installation of a beam gate prior to the second deceleration cavity (cf. Fig. 1)) together with a suitable combination of delay and pulse width of the switched deceleration potential made it possible to obtain a clean spectrum of one-cluster species only.

Fig. 3 shows a time-of-flight ion-cyclotron resonance of $^{12}C_{20}^+$ which was recorded with the channeltron ion detector (TOF detector above precision Penning trap in Fig. 1). Two types of detectors are in use at the ISOLTRAP experiment, either a microchannel plate (MCP) [23] or a channeltron ion detector [24]. The former has a diameter of $d_{MCP} = 5$ cm, a detection efficiency of 30%, and is mainly used for beam tuning and diagnostics. The latter has an aperture of $d_{chann} = 1$ cm. In this case, the detection efficiency was a factor of two higher compared to the MCP detector. Difficulties in beam focusing most probably are responsible for not reaching a detection efficiency of 90% demonstrated in earlier tests [24]. About 1500 ions of the carbon cluster $^{12}C_{20}^+$ were recorded with an excitation time of 1.2 s. The solid line is a fit to the data with the theoretical line shape [18], from which the cyclotron frequency could be determined to 377391.888(12) Hz. With the cluster $^{12}C_{10}^+$ as reference ion, the frequency ratio was determined according to Eq. (2) to $r = \nu_c^{ref}/\nu_c = 2.00000462(7)$. The measurement agrees with the defined mass within its uncertainty. The

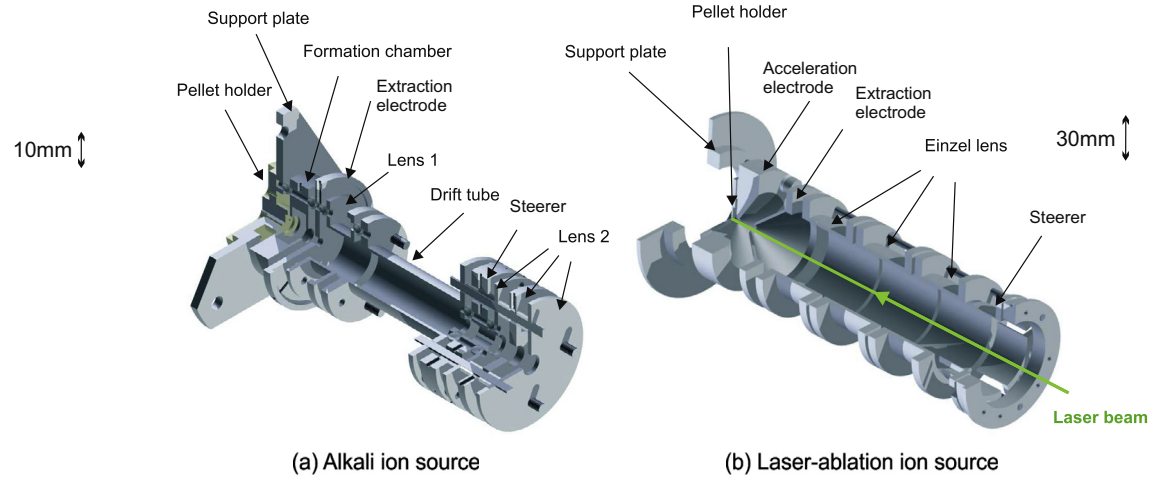

Fig. 2. Sectional view of the off-line ion sources of the ISOLTRAP experiment: The alkali ion source is shown on the left. The laser-ablation ion source is shown on the right. The drawing of each source includes the ionizer pellet and its corresponding mount, extraction geometry, and optical elements to guide the beam.

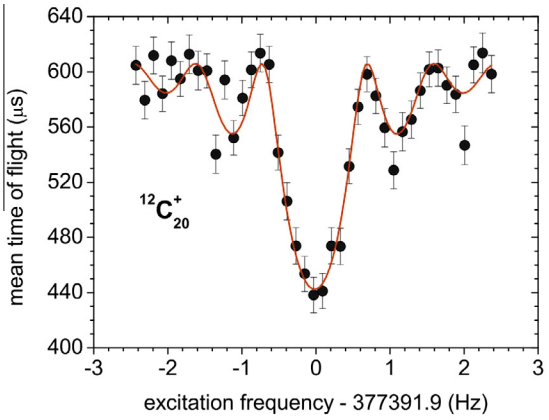

Fig. 3. Time-of-flight ion-cyclotron resonance of the cluster $^{12}C^{+}_{20}$ (dots). The time of flight of the ions to the detector is plotted as a function of the excitation frequency. The solid line is a fit of the theoretical line shape to the data [18].

availability of reference masses heavier than ^{133}Cs for measurements in the heavy-mass region of the nuclear chart becomes important to keep the mass-dependent uncertainty negligible.

3. Improved techniques for mass measurements and beam purification

The time-of-flight ion-cyclotron-resonance technique has been the method of choice for the precise mass measurement of radioactive nuclides for over two decades [19]. Routinely reaching relative statistical uncertainties on the order of 10^{-8}, the development of more refined measurement techniques for studying more exotic and shorter-lived nuclides constitutes a challenge. Recently, focus has been laid on either improving the achievable uncertainty or the suppression of isobaric contaminants.

3.1. Improved techniques for mass measurements

Compared to the Fourier-transform ion-cyclotron-resonance (FT-ICR) technique using resonance circuits [25,26], the TOF-ICR technique is universal for cyclotron frequency measurements in the sense that the detection electronics do not need to be rebuilt for each new ion species under investigation. Similar to the FT-ICR method, which can probe a single particle until its decay or loss from the trap using narrow-band, cryogenic detection circuits, the TOF-ICR technique is also based on single-ion detection. Yet, to complete a full measurement, i.e. to obtain a resonance, the frequency of the RF field exciting the ions has to be scanned. In this way, some few hundred ions are usually required to achieve a relative statistical uncertainty on the order of 10^{-8} within a measurement time of about one hour. Under certain conditions, results with higher precision have been accomplished [27,28]. Ramsey's idea of time-separated oscillatory fields offers an enhancement compared to the conventional TOF-ICR technique which can be exploited in two different ways. On the one hand, a statistical uncertainty reduced by a factor of 3–4 can be obtained within the same measurement time. On the other hand, comparable accuracy can be achieved within a tenth of the regular measurement time or with just one tenth of the recorded ions. The latter is of great relevance for the study of very short-lived radioactive nuclides, the former is interesting especially for experiments aiming at tests of fundamental symmetries or theories.

Although the so-called Ramsey excitation had already been proposed and demonstrated on stable ions in 1992 [29], the first successful measurement on radioactive ions, including a theoretical description, became available only in 2007 [30,31]. The resonance shown in the inset of Fig. 1 was taken during the on-line experiment on ^{82}Zn, which has a half-life of 228(10) ms [32]. Using a Ramsey excitation pattern of two excitation pulses with a length of 20 ms, which are separated by a waiting time of 160 ms (20-160-20), and with less than 100 ions distributed over 41 frequency steps, a relative statistical uncertainty of less than 10^{-7} could be achieved within a measurement time of only 45 min. The cyclotron frequency resulting from the fit of the theoretical line shape to the resonance in Fig. 1 is $\nu_c = 1107794.3(1)$ Hz. Table 1 compares the characteristics of this resonance to one of the conventional TOF-ICR spectra from which a factor of 5 gain in measurement time becomes evident. These two resonances had been combined with additional measurements to obtain the precise mass value quoted in [2].

Table 1
Characteristics of Ramsey excitation compared to conventional TOF-ICR excitation for the mass measurement of ^{82}Zn.

	TOF-ICR	
Characteristics	conventional	Ramsey
measurement time	195 min.	45 min.
excitation time	200 ms	(20–160-20) ms
ion count	580	80
relative uncertainty	$1 \cdot 10^{-7}$	$9 \cdot 10^{-8}$

3.2. Purification of samples

The radioactive ion beam delivered by the ISOLDE separator magnets (mass-resolving power on the order of $R \approx 10^3$) passes an aperture (the so-called slits) and may contain different species with atomic masses close to the ion of interest. What enters the ISOLTRAP setup is thus often a mixture of isobars or molecular quasi-isobars, which undergoes a first purification step in the MR-TOF MS reaching resolving powers on the order of $R \approx 10^5$. The mass-selective resonant buffer-gas centering has for many years been the method of choice for preparing a purified sample in a Penning trap [15] yielding similar resolving powers while simultaneously reducing the amplitudes of the three eigenmotions in the trap. Compared to isobar separation in the MR-TOF MS, however, this method requires some hundreds of milliseconds instead of only a few tens of milliseconds. The MR-TOF MS and applications will be discussed in detail in Section 4.

After the promising results of octupolar excitation [28,33–35], it was investigated whether the use of octupolar excitation can yield higher resolving power when applied to the mass-selective resonant buffer-gas centering method. The achievable resolving power was studied as a function of gas pressure, excitation duration and amplitude. In comparison with simulations including a binary-collision model, it could be shown that higher resolving powers are possible only at lower pressures than those typically used in the experiment. Since this is accompanied by increased measurement times due to a less efficient cooling process, it is not favorable to employ the octupolar excitation scheme for short-lived nuclides [36].

Another method is the so-called SIMCO excitation, which does not rely on a buffer-gas environment and was introduced in 2012 [37,38]. By simultaneous dipolar excitation of the magnetron motion and resonant quadrupolar excitation for the conversion between magnetron and cyclotron motion, a mass-selective re-centering of the ions of interest is performed while the contaminant ions are kept on a high magnetron radius and cannot exit the trap. First test measurements using a single-species ensemble of ions could demonstrate an ion efficiency above 90% and resolving

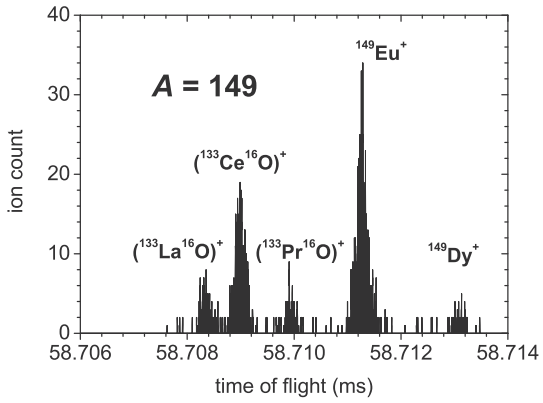

Fig. 4. MR-TOF spectrum of $A = 149$ isobars. The beam was produced using a tantalum target with a tungsten surface ion source.

powers in excess of 7×10^5. The SIMCO excitation scheme behaves robustly up to a few hundred trapped ions. In the future, the applicability of the SIMCO excitation for precision mass measurements will be studied.

The conventional technique for challenging cases of contaminations has been the dipole-cleaning technique, which can be employed in the high-vacuum environment of the precision Penning trap [39]. To this end, a dipolar RF field at the modified cyclotron frequency of the contaminating ion is applied with such a high amplitude that the ion moves on a high-radius cyclotron orbit and cannot be ejected from the trap. This method has demonstrated resolving powers beyond $R = 10^6$ on $^{195}Bi^+$ with a half-life of the two nuclear states on the order of $t_{1/2} \approx 100$ s, and can be performed on time scales ranging from a few hundred milliseconds to some seconds [40]. Application of this method removes even isomeric states from the trap center, leaving an isomerically pure sample for mass-spectrometry or decay-spectroscopy purposes [10]. In addition, experiments at JYFLTRAP have successfully used the Ramsey-cleaning method to separate isomers [41,42]. At LEBIT, the SWIFT (stored wave form inverse Fourier transform) technique has been demonstrated [43,44]. Very recently, the phase-imaging ion-cyclotron-resonance technique (PI-ICR) has been successfully tested at SHIPTRAP on ions from a reference source achieving resolving powers on the order of 10^8 [45]. It remains to be seen how this technique can be employed for purification.

4. The MR-TOF MS as a diagnostic tool

The optimization of the conditions for ion production and separation at ISOLDE is essential for the success of on-line experiments [46]. Experiments on radioactive beams usually require exact knowledge of the beam constituents. The ion-production conditions, as well as the separator magnet, are set up and then optimized to enhance the yield of the ion of interest and suppress the contaminating isobars as much as possible. For the recent experiment, which resulted in the mass measurement of ^{82}Zn [2], state-of-the art developments of ion-beam production at ISOLDE could be exploited: a neutron converter [47] and a quartz transfer line [48] for suppressing the rubidium and gallium contamination. The multi-reflection time-of-flight mass separator of ISOLTRAP has also decisively contributed to the success of the experiment through its outstanding isobaric purification and suppression on time scales an order of magnitude faster than conventional methods [9].

By reflection of the beam between electrostatic mirrors, a time-of-flight spectrum obtained from the MR-TOF MS together with an ion detector (MR-TOF detector in Fig. 1) can be converted into a mass spectrum using well-known calibrant ions. This method allows assigning mass-over-charge values to every flight time. Therefore, the MR-TOF MS can be used for precision mass measurements on nuclides with millisecond half-lives and minute production rates [12,49]. An additional application, which will be shown in the following, is the identification of the isobaric ion species in the ISOLDE beam using the MR-TOF MS. Exploiting also the mass-resolving power of the MR-TOF MS, this allows performing isotope-specific yield studies in connection with the different parameters for ion production and purification at ISOLDE.

4.1. Ion-beam yield analysis

The optimization of specific parameters relevant for ion production is an integral part of the Target-and-Ion-Source Development (TISD) program at ISOLDE [50]. This includes the investigation of production cross section, effusion and diffusion behavior, as well as ionization efficiency. Most of the time, these parameters can only be assessed during proton irradiation of the ISOLDE targets. The overall production rate as a function of target temperature, for example, is currently monitored using Faraday cups, while the identification of the ions of interest is performed by β and γ spectroscopy. The applicability is limited by the measurable ion count on the order of one pA, the branching ratio of the respective decays, the half-life of the ion of interest as well as background and detection efficiency.

The isobaric species of the ISOLDE beam appear as distinct time-of-flight peaks in the MR-TOF spectra recorded with the the MR-TOF detector of the ISOLTRAP experiment, as shown in Fig. 4 for the case of some $A = 149$ isobars. The beam was produced using a tantalum target with a tungsten ion source. Usually, the most prominent peak in the spectrum can easily be identified based on the calibration with off-line reference ions, and the relative distances to the neighboring time-of-flight signals can be used to further identify the ion ensemble [12]. In this way, the MR-TOF spectrum can be used to analyze the qualitative as well as quantitative composition of an unknown ion beam. The scattered counts arise from ions which were not properly cooled in the RFQ or which have been scattered due to imperfection in the MR-TOF injection. In general, the abundance ratios of the different species represent the ion-beam composition delivered from ISOLDE folded with possible half-life, charge-exchange loss or molecular break-up origination from buffer-gas collisions during the accumulation time in the RFQ. To derive absolute yield numbers, the efficiency of the ISOLTRAP setup up to the MR-TOF MS is calibrated via the signal intensity of a reference beam. Typical efficiencies lie on the order of one to a few percent. The advantages of ion-beam yield analysis using an MR-TOF MS constitute the measurement time on the order of 10 ms, direct ion detection, non-scanning operation, resolving power on the order of 10^5, and no dependence on decay properties (or resulting half-life limitations).

Once the isobaric composition of the beam is identified, each peak in the MR-TOF spectrum can be monitored individually and respective yield changes can be observed relative to ISOLDE ion-production and separation parameters, such as target and transfer line temperatures, delay from proton impact to the opening of the ISOLDE beam gate, or position of the separator slits. As an example, an MR-TOF spectrum at mass number $A = 149$ is shown in Fig. 4. Apart from the main peak of $^{149}Eu^+$ and some dysprosium ions, three oxides could be identified in the spectrum, based on the best agreement between the expected and measured time of flight in the MR-TOF spectrum, as well as considerations related to respective cross sections and chemistry of ion-production: $^{133}LaO^+$, $^{133}CeO+$, and $^{133}PrO^+$.

These measurements were performed within the ISOLDE experiment IS528 for cancer therapy [51]. The element terbium is the

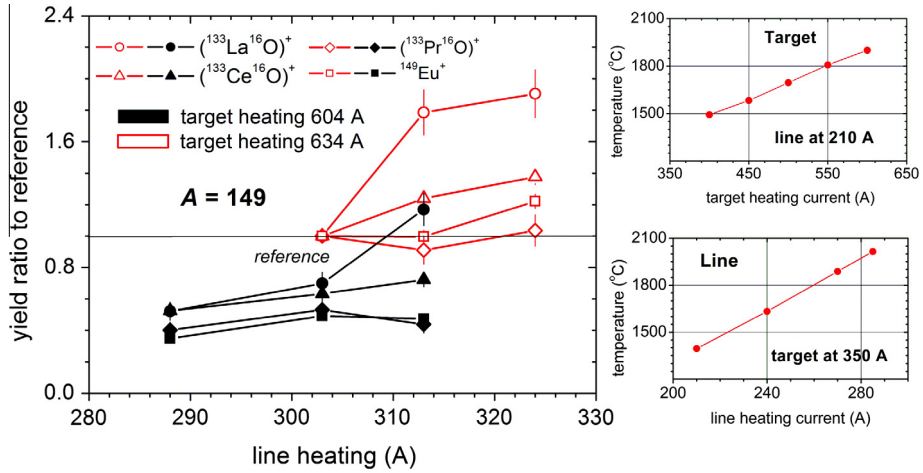

Fig. 5. Evolution of yield of the ion species shown in Fig. 4 as a function of transfer line heating for two different target temperatures. Marked in red are the data points for a target heating current of 634 A, marked in black for a target heating current of 604 A. The calibration curves of the transfer line and target temperatures as a function of the heating current are shown on the right. Solid lines are drawn to guide the eye.

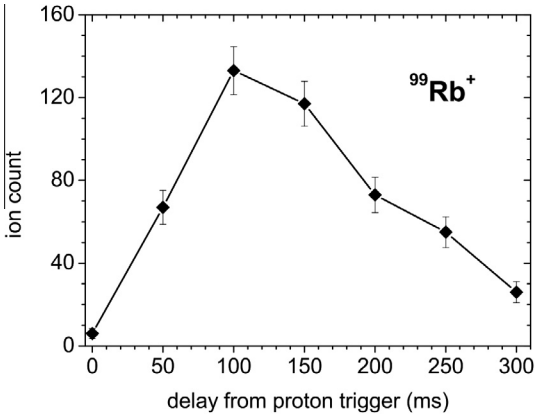

Fig. 6. Release curve of $^{99}Rb^{+}$ ($t_{1/2} = 54(4)$,ms), obtained with the MR-TOF MS by varying the delay between the proton impact and the opening of the ISOLDE beam gate. The solid line is drawn to guide the eye.

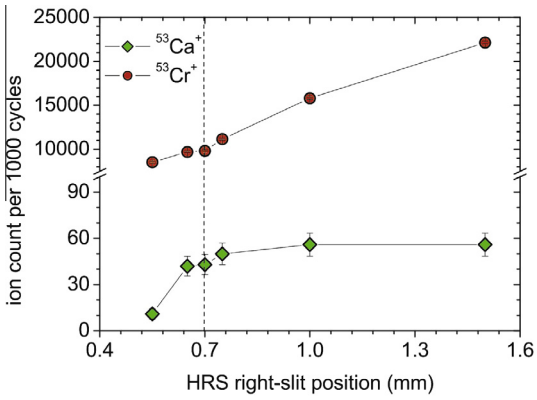

Fig. 7. Ion count detected at the ion detector behind ISOLTRAP's MR-TOF MS for the $A = 53$ isobars of Cr^{+} and Ca^{+} as a function of slit position. The dashed line marks the optimum yield ratio, the solid lines are drawn to guide the eye. For details, see text.

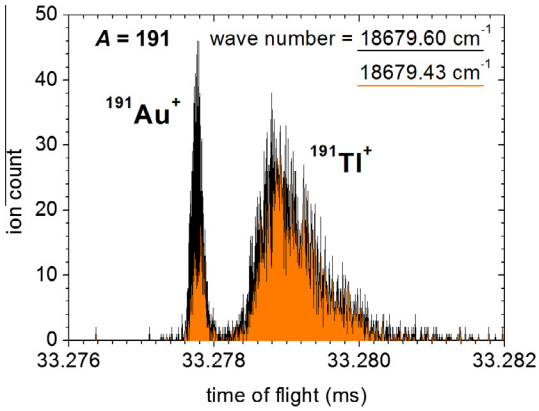

Fig. 8. MR-TOF spectrum of the ISOLDE beam at mass $A = 191$, for two different frequencies of the first RILIS excitation step. Only the laser-ionized ^{191}Au rate is dependent on the laser frequency. The ion count for optimized lasers is $N^{Au}_{opt} = 7035$, for detuned lasers $N^{Au}_{det} = 2981$.

only element in Mendeleev's table offering four clinically interesting radioisotopes with complementary nuclear decay characteristics covering all nuclear-medicine modalities [52]. Neutron-deficient Tb isotopes have to be produced at accelerators such as ISOLDE, where the mass-separated ion beams of the required radioisotopes can be collected. The aim of this measurement was to determine whether the direct laser ionization of Tb [53] or the laser ionization of Dy (with subsequent decay into Tb) provided a higher yield of Tb. As the beam composition on mass 149 is dominated by oxide sidebands, the quantification of the Dy/Tb yield by Faraday-cup measurements or γ-ray spectrometry is hindered.

Using the MR-TOF MS, a measurement of the yield dependence on target and transfer line temperature was performed by measuring the respective beam composition. The transfer line temperature was changed for two different target temperatures to see how the yield of the contaminating isobars could be manipulated to favor a high Dy/contamination ratio, which can be seen from Fig. 5. Here, the yield ratio to certain reference target and transfer-line-heating conditions are displayed, in red for a target heating current of 634 A, in black for a target heating current of 604 A. The variation in target heating of 30 A corresponds to 60° C at an absolute temperature of roughly 2000° C, cf. upper right plot of Fig. 5. The variation in transfer-line heating from 288 A to 324 A corresponds to 300° C at an absolute temperature of roughly 2000° C, cf. lower right plot of Fig. 5. The yield of the $A = 149$ isobars for a transfer-line-heating current of 303 A, a target heating current

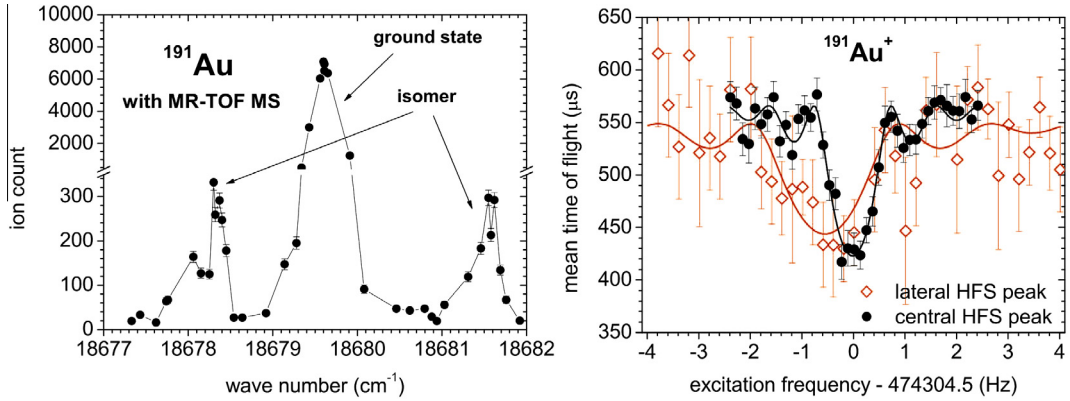

Fig. 9. The ^{191}Au TOF-gated ion-count rate at the MR-TOF detector as a function of the laser frequency of first excitation step of the Au ionization scheme. The central peak (lateral peaks) corresponds to ions in the ground (excited) state of ^{191}Au. TOF-ICR spectrum of ground (black points) and isomeric (red diamonds) state of ^{191}Au. The spectra could be obtained by tuning the laser frequency of RILIS to one of the isomeric HFS peaks.

of 634 A, and a proton intensity of 1.9 μ A was taken as reference (solid line of Fig. 5).

The release time of radioactive isotopes from ISOL targets is strongly dependent on the chemical properties, as well as on the target material, temperature and degradation caused by proton impact. The ratio between a contaminant and the ion of interest can in certain cases be reduced by sampling the radioactive beam (i.e. opening the ISOLDE beam gate) only after each proton impact on target, with an optimized delay, which depends on the release properties of both species. Knowing the release properties of the ion of interest and of the major contaminants is thus important for improving yield and purity of the beam, especially when the ion of interest has a short half-life. Using the resolved TOF spectrum on the MR-TOF detector (cf. Fig. 1) and varying the time between proton impact and opening of the ISOLDE beam gate, the time structure of the release can be determined for the ion of interest and for its contaminants, as shown in Fig. 6 for the case of the short-lived isotope ^{99}Rb with a half-life of only $t_{1/2} = 54(4)$ ms [54].

During the measurement of neutron-rich calcium isotopes within the ISOLDE experiment IS532 [55], the isobaric mixture delivered from ISOLDE had a high contribution of stable chromium. The measurement of ^{53,54}Ca [49] was rendered possible by carefully tuning the ion-count ratio of the main contaminant with respect to the calcium yield. Exploiting the low resolving-power requirement of only $R \approx 1800$ between Ca and Cr, the yield of the contaminant could be varied by changing the size of the aperture behind the high-resolution separator (HRS) magnet used for this experiment. Fig. 7 shows the yields at the MR-TOF detector as a function of the position of the right slit of the HRS. The yield of the two isobars was recorded for 1000 measurement cycles, a cycle being the time from opening of the ISOLDE beam gate until detection at the MR-TOF detector. Upon decreasing the aperture, i. e. mechanically moving the right slit towards the beam axis at 0 mm, the calcium yield stayed constant while the chromium yield started decreasing. The slit position of 0.7 mm marks the best ratio without significant losses of calcium. The yield ratio of originally more than 500 could be reduced to approximately 250.

4.2. Analysis of isomeric states

If the energy difference between a nuclear ground state and isomer is large, the purification techniques described in Section 3 may have sufficient resolving power to separate these states. If this is not the case, a different approach is to attempt isomer selection at the ionization stage of beam production. The Resonance Ionization Laser Ion Source (RILIS) of ISOLDE uses the highly selective ionization technique of multi-step resonance excitation of atoms [56]. The ability to enable or cease the resonant ionization process by irradiating or blocking the laser beams enables unambiguous identification of the laser ionized component of the ion beam. Despite the large line width (1–20 GHz) of the tunable lasers and the Doppler broadening of the atomic transitions in the hot-cavity ionization region, the RILIS lasers can probe the large hyperfine splitting of atomic transitions that occur for some elements. In certain cases, respective tuning of the wavelength of one of the steps in the laser-ionization scheme can result in preferential ionization of a nuclear ground state or isomer [57,58].

Examples of how resonance laser ionization in combination with Penning-trap mass spectrometry led to the unambiguous identification of long-lived nuclear states and their ordering are the ones of ^{68,70}Cu, experiments which were conducted at ISOLDE involving RILIS and ISOLTRAP [59,60]. The laser frequency of RILIS could be tuned in such a way as to ionize mainly one of the three isomers. A subsequent mass measurement of the sample using the TOF-ICR technique led to the identification of ground and isomeric states. The MR-TOF MS can assist with the optimization of this wavelength tuning by TOF separation of the surface and laser-ionized components of the ion beam. It therefore provides a background-free means of detecting the photo-ions whilst the laser is scanned across the hyperfine structure of the atomic transition.

Fig. 8 shows the separation of the ^{191}Au and ^{191}Tl components of the ISOLDE beam in the MR-TOF spectrum. The laser ionized Au component is identified by its dependence on the frequency tuning of the respective RILIS laser[1]. Please note that the large peak width of the Tl peak compared to the Au peak most likely comes from the Tl ions being located at the edges of the pulsed cavity upon switching. In the case of ^{191}Au, the ground and an isomeric state are separated by 266.3(4) keV [61] and thus cannot be easily separated by their time of flight in the MR-TOF MS. The hyperfine splitting of the isomeric state, however, is much larger than that of the ground state. Fig. 9 shows on the left the number of ions counted at the MR-TOF detector (cf. Fig. 1) as a function of the frequency of the first RILIS excitation step. The central peak corresponds to ions in the ground state of ^{191}Au, the lateral peaks belong to ^{191m}Au. Precise tuning of the laser wavelength in this way provided an isomerically pure sample to be sent to the Penning traps of the ISOLTRAP experiment. The TOF-ICR technique was used subsequently to perform mass measure-

[1] Since the frequency was recorded in the unit of inverse centimeters, the corresponding label "wave number (cm^{-1})" will be used for graphical representation throughout the paper.

ments of the two states, which can be seen from Fig. 9, right side. The black points (red diamonds) correspond to the ground (isomeric) state. The yield of the ground state ($t_{1/2} = 3.18$ h) was about one order of magnitude higher than that of the isomer ($t_{1/2} = 920(110)$ ms [61]). The resonance peak is narrower, because a 1.2-s excitation time could be used. Fitting the theoretical line shape to the resonance, a cyclotron frequency for $^{191}Au^+$ of $\nu_c = 474304.48(2)$ Hz could be determined. With $^{133}Cs^+$ as reference ion, the frequency ratio was determined following Eq. (2) to $r = \nu_c^{ref}/\nu_c = 1.43684065(4)$, yielding a mass excess of $-33797.7(4.9)$ keV. Due to the very low production rate and the much shorter half-life of the isomeric state, the signal-to-noise ratio is decreased compared to the resonance of the ground state. Low statistics and large scattering hindered a precise determination of the baseline. The resonance of the isomeric state was taken with an excitation time of 600 ms, from which the excitation energy of the ^{191}Au isomer was determined to $E_{ex} = 210(56)$ keV. This is in agreement with the literature value of $E_{ex}^{lit} = 266.3(4)$ keV [61] corroborating the association to the corresponding peak in the Au hyperfine structure.

The example of ^{191}Au illustrates that the MR-TOF MS together with an ion detector can help to investigate the hyperfine structure of radioactive isotopes. In certain cases, it offers the necessary information for providing isomerically pure beams, which in turn can be made available for different experiments.

5. Conclusion

The technical developments of the mass spectrometer ISOLTRAP have been presented. They illustrate new perspectives for Penning-trap mass spectrometry. Regarding their benefits for a mass-measurement program, the possibilities can be divided into three groups. First, developments like new excitation schemes aim at reducing the achievable measurement uncertainty or enhancing the resolving power. Second, efforts have been made to ensure a fast measurement process, which becomes critical for radisotopes with shorter half-lives and lower production rates. Third, examples of enhanced background suppression through separation have been discussed where measurements became feasible which otherwise would have been impossible due to the contamination in the radioactive ion beam. The application of the MR-TOF MS as a mass spectrometer for mass measurements on rare exotic nuclides, combined with a highly-selective ionization technique for the identification of the ion of interest, will become crucial. Another field of interest, which has been demonstrated on radioactive ion beams, is the use of the MR-TOF MS in combination with an ion detector for ion-beam analysis. There are numerous applications aiming at the identification of the beam constituents and the optimization of beam production and purification, including isomeric purification by (hyperfine-structure-based) selective ionization. The main advantages provided by the MR-TOF MS are background suppression for performing isotope-specific studies, such as yield optimization and laser spectroscopy, direct ion detection, and no dependence on the decay properties of the ion of interest. Currently, ISOLTRAP's MR-TOF MS is the only multi-reflection time-of-flight mass separator routinely working on radioactive samples. Two other machines are being tested at GSI and at RIKEN [62,63], other facilities are currently investigating the implementation of similar devices. As beam analyzer and purifier, multi-reflection time-of-flight mass separators have great potential at radioactive ion-beam facilities to serve the different experimental setups.

Acknowledgements

We thank B. Marsh for comments on the manusript and S. Rothe for discussions. This work was supported by the BMBF under Contracts No. 05P12HGCI1, 05P12HGFNE, 05P09ODCIA, the EU through ENSAR (Grant No. 262010), the French IN2P3, the ISOLDE Collaboration, and the Max-Planck Society. S. Kreim acknowledges support from the Robert-Bosch Foundation.

References

[1] H.-J. Kluge, Penning trap mass spectrometry of radionuclides, Int. J. Mass Spectrom. 349 (2013) 26.
[2] R.N. Wolf, D. Beck, K. Blaum, Ch. Böhm, Ch. Borgmann, M. Breitenfeldt, N. Chamel, S. Goriely, F. Herfurth, M. Kowalska, S. Kreim, D. Lunney, V. Manea, E. Minaya Ramirez, S. Naimi, D. Neidherr, M. Rosenbusch, L. Schweikhard, J. Stanja, F. Wienholtz, K. Zuber, Phys. Rev. Lett. 110 (2013) 041101.
[3] S. Kreim, M. Hempel, D. Lunney, J. Schaffner-Bielich, Int. J Mass Spectrom. 349 (2013) 63.
[4] K. Blaum, J. Dillling, W. Nörtershäuser, Phys. Scr. T152 (2013) 014017.
[5] A. Kankainen, J. Äystö, A. Jokinen, J. Phys. G 39 (2012) 093101.
[6] M. Kowalska et al., ISOLTRAP results 2006–2009, Hyp. Int. 196 (0304–3843) (2010) 199.
[7] E. Kugler et al., Hyp. Int. 129 (2000) 23.
[8] M. Mukherjee, D. Beck, K. Blaum, G. Bollen, J. Dilling, S. George, F. Herfurth, A. Herlert, A. Kellerbauer, H.-J. Kluge, S. Schwarz, L. Schweikhard, C. Yazidjian, Eur. Phys. J. A. 35 (2008) 1.
[9] R.N. Wolf, D. Beck, K. Blaum, C. Böhm, C. Borgmann, M. Breitenfeldt, F. Herfurth, A. Herlert, M. Kowalska, S. Kreim, D. Lunney, S. Naimi, D. Neidherr, M. Rosenbusch, L. Schweikhard, J. Stanja, F. Wienholtz, K. Zuber, Nucl. Instrum. Methods A 686 (2012) 82.
[10] M. Kowalska, S. Naimi, J. Agramunt, A. Algora, D. Beck, B. Blank, K. Blaum, C. Böhm, C. Borgmann, M. Breitenfeldt, L.M. Fraile, S. George, F. Herfurth, A. Herlert, S. Kreim, D. Lunney, E. Minaya-Ramirez, D. Neidherr, M. Rosenbusch, B. Rubio, L. Schweikhard, J. Stanja, K. Zuber, Nucl. Instrum. Methods A 689 (2012) 102.
[11] F. Herfurth, J. Dilling, A. Kellerbauer, G. Bollen, S. Henry, H.-J. Kluge, E. Lamour, D. Lunney, R.B. Moore, C. Scheidenberger, S. Schwarz, G. Sikler, J. Szerypo, Nucl. Instrum. Methods A 469 (2001) 254.
[12] R.N. Wolf, F. Wienholtz, D. Atanasov, D. Beck, K. Blaum, C. Borgmann, F. Herfurth, M. Kowalska, S. Kreim, Y. Litvinov, D. Lunney, V. Manea, D. Neidherr, M. Rosenbusch, L. Schweikhard, J. Stanja, K. Zuber, Int. J. Mass Spectrom. 349 (2013) 123.
[13] R.N. Wolf, G. Marx, M. Rosenbusch, L. Schweikhard, Int. J. Mass. Spectrom 313 (2012) 8.
[14] N. Bradbury, R. Nielsen, Phys. Rev. 49 (1936) 388.
[15] G. Savard, S. Becker, G. Gollen, H.-J. Kluge, R.B. Boore, T. Otto, L. Schweikhard, H. Stolzenberg, U. Wiess, Phys. Lett. A 158 (1991) 247.
[16] L.S. Brown, G. Gabrielse, Rev. Mod. Phys. 58 (1986) 233–311.
[17] G. Gräff, H. Kalinowsky, J. Traut, Z. Phys. A 297 (1980) 35.
[18] M. König, G. Bollen, H.-J. Kluge, T. Otto, J. Szerypo, Int. J. Mass. Spectrom. Ion Process. 142 (1995) 95.
[19] G. Bollen, R.B. Moore, G. Savard, H. Stolzenberg, J. Appl. Phys. 68 (1990) 4355.
[20] K. Blaum, G. Bollen, F. Herfurth, A. Kellerbauer, H.-J. Kluge, M. Kuckein, E. Sauvan, C. Scheidenberger, L. Schweikhard, Eur. Phys. J. A 15 (2002) 245.
[21] D. Fink, J. Barea, D. Beck, K. Blaum, C. Böhm, C. Borgmann, M. Breitenfeldt, F. Herfurth, A. Herlert, J. Kotila, M. Kowalska, S. Kreim, D. Lunney, S. Naimi, M. Rosenbusch, S. Schwarz, L. Schweikhard, F. Simkovic, J. Stanja, K. Zuber, Phys. Rev. Lett. 108 (2012) 062502.
[22] J.R. Pierce, Theory and design of electron beams, Van Nostrand, 1949.
[23] J.L. Wiza, Nucl. Instrum. Methods 162 (1979) 587.
[24] C. Yazidjian, K. Blaum, R. Ferrer, F. Herfurth, A. Herlert, L. Schweikhard, Hyp. Int. 173 (2006) 181.
[25] H.G. Dehmelt, F.L. Walls, Phys. Rev. Lett. 21 (1968) 127.
[26] D.J. Wineland, H.G. Dehmelt, J. Appl. Phys. 46 (1975) 919.
[27] S. Nagy, T. Fritioff, A. Solders, R. Schuch, M. Björkhage, I. Bergström, Eur. Phys. J. D. 39 (2006) 1.
[28] S. Eliseev, C. Roux, K. Blaum, M. Block, C. Droese, F. Herfurth, M. Kretzschmar, M.I. Krivoruchenko, E. Minaya-Ramirez, Y.N. Novikov, L. Schweikhard, V.M. Shabaev, F. Simkovic, I.I. Tupitsyn, K. Zuber, N.A. Zubova, Phys. Rev. Lett. 107 (2011) 152501.
[29] G. Bollen, H.-J. Kluge, T. Otto, G. Savard, H. Stolzenberg, Nucl. Instrum. Methods B 70 (1992) 490.
[30] S. George, S. Baruah, B. Blank, K. Blaum, M. Breitenfeldt, U. Hager, F. Herfurth, A. Herlert, A. Kellerbauer, H.-J. Kluge, M. Kretzschmar, D. Lunney, R. Savreux, S. Schwarz, L. Schweikhard, C. Yazidjian, Ramsey Method of Separated Oscillatory Fields for High-Precision Penning Trap Mass Spectrometry, Phys. Rev. Lett. 98 (16) (2007) 162501.
[31] M. Kretzschmar, Int. J. Mass Spectrom. 264 (2007) 122.
[32] M. Madurga, I.N. Borzov, R. Surman, R. Grzywacz, K.P. Rykaczewski, C.J. Gross, D. Miller, D.W. Stracener, J.C. Batchelder, N.T. Brewer, L. Cartegni, J.H. Hamilton, J.K. Hwang, S.H. Liu, S.V. Ilyushkin, C. Jost, M. Karny, A. Korgul, W. Królas, A. Kuźniak, C. Mazzocchi, K. Miernik, S.W. Padgett, S.V. Paulauskas, A.V. Ramayya, J.A. Winger, M. Wolińska-Cichocka, E.F. Zganjar, Phys. Rev. Lett. 109 (11) (2012) 112501.
[33] S. Eliseev, M. Block, A. Chaudhuri, F. Herfurth, H.-J. Kluge, A. Martin, C. Rauth, G. Vorobjev, Int. J. Mass Spectrom. 262 (2007) 45.

[34] R. Ringle, G. Bollen, P. Shury, S. Schwarz, T. Sun, Int. J. Mass Spectrom. 262 (2007) 33.
[35] M. Breitenfeldt, F. Ziegler, A. Herlert, G. Marx, L. Schweikhard, Int. J. Mass Spectrom. 263 (2007) 294.
[36] M. Rosenbusch, C. Böhm, C. Borgmann, M. Breitenfeldt, A. Herlert, M. Kowalska, S. Kreim, G. Marx, S. Naimi, D. Neidherr, R. Schneider, L. Schweikhard, Int. J. Mass Spectrom. 314 (2012) 6.
[37] M. Rosenbusch, K. Blaum, C. Borgmann, S. Kreim, M. Kretzschmar, D. Lunney, L. Schweikhard, F. Wienholtz, R.N. Wolf, Int. J. Mass Spectrom. 325 (2012) 51.
[38] M. Kretzschmar, Int. J. Mass Spectrom. 325 (2012) 30.
[39] P. Becker, G. Bollen, F. Kern, H.-J. Kluge, R.B. Moore, G. Savard, L. Schweikhard, H. Stolzenberg, Mass measurements of very high accuracy by time-of-flight ion cyclotron resonance of ions injected into a penning trap, Int. J. Mass Spectrom. 99 (0168–1176) (1990) 53–77.
[40] C. Weber, G. Audi, D. Beck, K. Blaum, G. Bollen, F. Herfurth, A. Kellerbauer, H.-J. Kluge, D. Lunney, L. Schweikhard, Nucl. Phys. A 803 (2008) 1.
[41] T. Eronen, V.-V. Elomaa, U. Hager, J. Hakala, A. Jokinen, A. Kainkainen, S. Rahaman, J. Rissanen, C. Weber, J. Aystö, Nucl. Instrum. Methods B 266 (2008) 4527.
[42] A. Kankainen, J. Hakala, T. Eronen, D. Gorelov, A. Jokinen, V.S. Kolhinen, I.D. Moore, H. Penttilä, S. Rinta-Antila, J. Rissanen, A. Saastamoinen, V. Sonnenschein, J. Äystö, Phys. Rev. C 87 (2013) 024307.
[43] S. Guan, A.G. Marshall, Int. J. Mass Spectrom. 157 (158) (1996) 5.
[44] M. Redshaw, et al., this volume (2013).
[45] S. Eliseev, K. Blaum, M. Block, C. Droese, M. Goncharov, E. Minaya Ramirez, D.A. Nesterenko, Yu.N. Novikov, L. Schweikhard, Phase-Imaging Ion-Cyclotron-Resonance Measurements for Short-Lived Nuclides, Phys. Rev. Lett. 110 (8) (2013) 082501.
[46] Y. Blumenfeld, T. Nilsson, P. Van Duppen, Phys. Scr. T152 (2013) 014023.
[47] U. Köster, Eur. Phys. J. A 15 (2002) 255.
[48] E. Bouquerel, R. Catherall, M. Eller, J. Lettry, S. Marzari, T. Stora, Nucl. Instrum. Methods B 266 (2008) 4298.
[49] F. Wienholtz, D. Beck, K. Blaum, C. Borgmann, M. Breitenfeldt, R.B. Cakirli, S. George, F. Herfurth, J.D. Holt, M. Kowalska, S. Kreim, D. Lunney, V. Manea, J. Menéndez, D. Neidherr, M. Rosenbusch, L. Schweikhard, A. Schwenk, J. Simonis, J. Stanja, R.N. Wolf, K. Zuber, Nature 498 (2013) 346.
[50] T. Stora, this volume (2003).
[51] H. Dorrer, C. Ghezzi, F. Haddad, M. Jensen, U. Koster, C. Müller, B. Pichler, A.M. Rolle, R. Schibli, J. Siikanen, Novel diagnostic and therapeutic radionuclides for the development of innovative radiopharmaceuticals, howpublishedCERN INTC Proposal, INTC-P-312, 2011.
[52] C. Müller, K. Thernosekov, U. Köster, K. Johnston, H. Dorrer, A. Hohn, N.T. Van der Walt, A. Türler, R. Schibli, J. Nucl. Med. 53 (2012) 1951.
[53] U. Köster, V.N. Fedoseyev, A.N. Andreyev, U.C. Bergmann, R. Catherall, J. Cederkäll, M. Dietrich, H. De Witte, D.V. Fedorov, L. Fraile, S. Franchoo, H. Fynbo, U. Georg, T. Giles, M. Gorska, M. Hannawald, M. Huyse, A. Joinet, O.C. Jonsson, K.L. Kratz, K. Kruglov, C. Lau, J. Lettry, V.I. Mishin, M. Oinonen, K. Partes, K. Präjärvi, B. Pfeiffer, H.L. Ravn, M.D. Seliverstov, P. Thirolf, K. Van de Vel, P. Van Duppen, J. Van Roosbroeck, L. Weissman, Nucl. Instrum. Methods B 204 (2003) 347.
[54] G. Audi, F.G. Kondev, M. Wang, B. Pfeiffer, X. Sun, J. Blachot, M. MacCormick, Chinese Phys. C 36 (2012) 1157.
[55] S. Kreim, D. Beck, K. Blaum, C. Böhm, C. Borgmann, M. Breitenfeldt, R.B. Cakirli, F. Herfurth, M. Kowalska, Y. Litvinov, D. Lunney, V. Manea, S. Naimi, D. Neidherr, M. Rosenbusch, L. Schweikhard, J. Stanja, T. Stora, F. Wienholtz, R.N. Wolf, K. Zuber, Seeking the purported magic number $N = 32$ with high-precision mass spectrometry, CERN INTC Proposal, INTC-P-317, 2011.
[56] V.N. Fedosseev, L.-E. Berg, D.V. Fedorov, D. Fink, O.J. Launila, R. Losito, B.A. Marsh, R.E. Rossel, S. Rothe, M.D. Seliverstov, A.M. Sjodin, K.D.A. Wendt, Rev. Sci. Instrum. 83 (2012) 02A903.
[57] V.N. Fedosseev, D.V. Fedorov, R. Horn, G. Huber, U. Köster, J. Lassen, V. Mishin, M.D. Seliverstov, L. Weissman, K.D.A. Wendt, Nucl. Instrum. Methods B 204 (2003) 353.
[58] B.A. Marsh, et al., this volume (2013).
[59] J. Van Roosbroeck, C. Guénaut, G. Audi, D. Beck, K. Blaum, G. Bollen, J. Cederkall, P. Delahaye, A. De Maesschalck, H. De Witte, D. Fedorov, V.N. Fedoseyev, S. Franchoo, H.O.U. Fynbo, M. Górska, F. Herfurth, K. Heyde, M. Huyse, A. Kellerbauer, H.-J. Kluge, U. Köster, K. Kruglov, D. Lunney, V.I. Mishin, W.F. Mueller, S. Nagy, S. Schwarz, L. Schweikhard, N.A. Smirnova, K. Van de Vel, P. Van Duppen, A. Van Dyck, W.B. Walters, L. Weissmannn, C. Yazidjian, Phys. Rev. Lett. 92 (2004) 112501.
[60] K. Blaum, D. Beck, G. Bollen, P. Delahaye, C. Guénaut, F. Herfurth, A. Kellerbauer, H.-J. Kluge, D. Lunney, S. Schwarz, L. Schweikhard, C. Yazidjian, Eur. Phys. Lett. 67 (2004) 586.
[61] H. Beuscher, P. Jahn, R.M. Lieder, C. Mayer-Boricke, Z. Phys. 247 (1971) 383.
[62] W. Plass, T. Dickel, C. Scheidenberger, Int. J. Mass Spectrom. 349 (2013) 134.
[63] P. Schury, K. Okada, S. Shehepunov, T. Sonoda, A. Takamine, M. Wada, H. Wollnik, Y. Yamazaki, Eur. Phys. J.A 42 (2009) 343.